Jurnal Teknologi

Full paper

Characterization of Human Head Phantom based on its Dielectric Properties for Wideband Microwave Imaging Application

Mohd Sollehudin Md Said[a], Norhudah Seman[a*], Haliza Jaafar[b]

[a]*Wireless Communication Centre (WCC), Universiti Teknologi Malaysia, 81310 UTM Johor Bahru, Johor, Malaysia*
[b]*Language Academy, Universiti Teknologi Malaysia, 81310 UTM Johor Bahru, Johor, Malaysia*

*Corresponding author: huda@fke.utm.my

Article history

Received : 15 August 2014
Received in revised form :
5 January 2015
Accepted : 10 February 2015

Graphical abstract

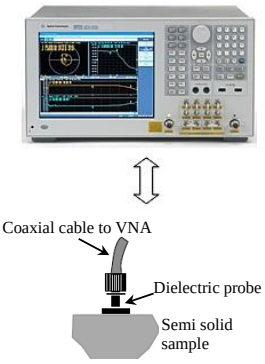

Abstract

Characterization of phantom material based on its electrical properties across 1 to 6 GHz is investigated and presented in purpose for modelling of a human head phantom. This article presents five phantom samples mimicking main head tissues, which are the tissue of grey matter, white matter, cerebral spinal fluid (CSF), blood and skin. The preparation of phantom samples is performed by using common and cheap materials, which are jelly powder, gelatine, water and sugar. The characteristics of materials used are discussed on the composition ratios and electrical properties. The electrical properties of materials are measured using a special dielectric coaxial probe connected to a vector network analyser (VNA). The obtained data is analysed in terms of relative permittivity, ε_r and conductivity, σ for the observation and further discussion on the characterizations. This phantom of the human head tissues later can be applied in the microwave imaging system for a further study on the health monitoring of the human body.

Keywords: Head; phantom; dielectric; microwave; imaging; wideband

1.0 INTRODUCTION

The potential use of microwave imaging in breast cancer imaging, has led to its great awareness and attention among researchers [1, 6-14]. Microwave imaging is reported to be an alternative imaging technique that is safe, portable and available at lower cost compared to existing imaging modalities [17]. Microwave imaging benefits from the tissue properties at microwave frequencies offer notable higher contrast than other techniques. This imaging applies a multi-static real aperture technique and advanced signal processing which provides good resolution to be clinically useful. Besides its application predominantly proposed for breast cancer detection, some interests have been reported on the use of microwave in extremity imaging, diagnostics of lung cancer, brain imaging and cardiac imaging [1-6]. Despite the interest in microwave imaging among researchers, (this?) research mostly focused on the numerical simulation with simple experimental works [2-5].

Therefore, in order to carry out a research in this area, multi-disciplinary effort is required. In the case of measurement, the physical human phantom is required to be developed and then illuminated by an antenna or array of antennas operating over the desired microwave frequency band. The reflected and transmitted signals collected by antennas can be stored for further processing. Depending on the processing technique chosen, this data can be efficiently used to produce a map of dielectric constant in an imaged body, such a work has been done on breast phantom that was reported in [7].

2.0 HUMAN HEAD IMAGING

Despite the great awareness and interest for microwave radiometry, most of the research is focusing on breast imaging [1, 6-14]. Recently, the microwave imaging for detection of brain abnormalities has been proposed in [17-22] that mostly done by the computed tomography (CT) and magnetic

resonance imaging (MRI) to overcome the complexity of stroke diagnosis. However, the CT and MRI scan systems are not fast, cost effective or portable, nor are accessible at rural medical clinics, or carried by first response paramedical teams [22]. In contrast, the microwave has potential for imaging that can be a supplement to current diagnostic methods as it may provide fast, cost-effective and portable detection system [17].

Brain imaging is considered a significantly more difficult application, mainly due to the complexity in terms of structural, functional and electrical properties in homogeneity of the human brain [24]. At microwave frequencies of 0.3 to 30 GHz, the brain is surrounded by a high-contrast dielectric shield comprising the skin, skull and cerebral spinal fluid (CSF). Therefore, determining the optimal spectrum in which to couple electromagnetic energy into the brain matter is extremely important [21]. At lower frequencies than 3 GHz, it would allow for a higher penetration but would be insensitive to small regions of dielectric changes [21]. Relatively, high microwave frequencies, such as those used in ultra-wideband breast cancer detection, has high resolution, although may lack the required penetration into the brain. In [17], a successful image reconstruction using a frequency range of 0.5–2 GHz has been applied with a circular object to represent a head. In the system, the response of the head model was placed on one focal point of the ellipsoidal cavity, while the excitation generated by a dipole antenna positioned on the other focus, which is calculated as reported in [18]. Hence, by referring to [15-24], the frequency range that is proposed to be applied in this research is 1 to 6 GHz in order to have good trade-off between resolution and penetration in human head imaging.

■3.0 ELECTRICAL PROPERTIES OF HUMAN TISSUES

The investigations of electrical properties of the human body are important in the analysis of medical applications. At this level, knowledge of the electrical properties can provide understanding of the elementary basis of biological processes. To investigate and analyse the electrical properties, the permittivity and conductivity data of the biological tissues are necessary. Basically, the possessions of the biological tissue can be separated into conducting and insulating type. For the conducting type, the natures of the electrical charge are free to move toward the application of an electrical field. While, for insulating type, the charges are bound and not free to move [25].

Actually, most materials, including biological tissues present the characteristics of both insulators and conductors because of the existence of dipoles. On a macroscopic level, the material is described as having a permittivity and conductivity. The permittivity characterizes the materials ability to store charge or to rotate molecular dipoles, while in contrast the conductivity describes the ability to transport charge. However, in physical terms, permittivity can be defined as the measured of the ability of dipoles to rotate or store charge by an applied external field. The conductivity, on the other hand, can be described as a measure of the ability of its charge to be transported throughout its volume by an applied electric field. In general, if the dielectric properties are at a constant level, the displacement current will increase proportionally to the frequency, whereas the conductivity current will remain unchanged [25].

The permittivity of free space is given as ε_0 = 8.85x 10^{-12} F/m. Hence, generally permittivity property of a material can be expressed as in Equation (1) [25]:

$$\varepsilon = \varepsilon_r \varepsilon_0 \quad (1)$$

where, ε_r is relative permittivity. Commonly, the permittivity is treated as a complex function of the frequency. Therefore, the complex permittivity, ε^* can be defined as [25]:

$$\varepsilon^* = \varepsilon_r' - j\frac{\sigma}{\omega\varepsilon_0} = \varepsilon_r' - j\varepsilon_r'' \quad (2)$$

where σ, ω, $\varepsilon_r'$and ε_r'' are conductivity, angular frequency, real part and imaginary part of permittivity, respectively. From the measured complex permittivity value in (2), the conductivity value can be obtained using (3):

$$j\frac{\sigma}{\omega\varepsilon_o} = j\varepsilon_r'' \quad (3)$$

Referring to (3), it shows that the conductivity is related to the imaginary part of complex permittivity. Therefore, the conductivity can be computed using (4):

$$\sigma = \varepsilon_r''\omega\varepsilon_o \quad (4)$$

■4.0 HUMAN HEAD PHANTOM

In order to develop the microwave imaging system, it is necessary to set-off the experiment by investigating and modelling a realistic brain phantom for a microwave imaging system. Therefore, to perform this experiment, it is important to have knowledge on the composition and electrical properties of a real human brain. In the past few years, the first modelling of the head phantom for microwave imaging started by monitoring human brain disease [31-32]. From reported work in [31], the head phantom is made using gelatine-based material that only focuses on single average head tissue that operated in frequency range from 1 to 4 GHz. While in [32], the head phantom is improved to be more realistic because they (were made from?) several brain tissues, which are grey matter, white matter and cerebral spinal fluid (CSF). Commonly the conducted works on the head phantom only focuses on the composition of material used as ingredients. Nevertheless, clear explanation on the characteristic properties of the material used is not provided. Thus, the study in this article focuses on a few types of human head tissues, which are grey matter, white matter, cerebral spinal fluid (CSF), blood, and skin tissues. In this research, the measurement is performed to determine the electrical properties of the assorted substances across the frequency band of 1 to 6 GHz for the modelling of a realistic human head phantom.

In conducting the experiment, two main substances that used are jelly powder and gelatine. Then, the other ancillary substances like water and/or sugar are mixed with one of the main substances in a certain ratio to produce the phantom samples for grey matter, white matter, cerebral spinal fluid (CSF), blood and skin tissues. The reasons why these main substances are chosen in this experiment are because they are available in a large amount in the market at low cost.

These substances also can be recognized as Lower Molecular Weight Gelators (LMWGs).The LMWGs are gelators that consist of organic compounds with a molecular weight of less than 2000 Da, which showing gelation behaviour in organic solvent and sometimes in water [27]. Hence, jelly and gelatine belong to a family of gels, which have properties between soft and hard depending on its composition. Where, gels can be recognized as semisolid or solid substance, which is basically from a liquid, than three-dimensional (3D) cross-linked networks that exist within the liquid which act as bonding

material that bond molecules of the liquid and force it to behave like a solid. Figure 1 shows the stages in the formation of a gel.

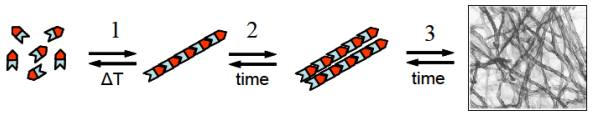

Figure 1 Schematic representation of the formation of a 3D-network starting from dissolved gelator molecules

At high level of temperature, molecules of gel completely dissolve as in Figure 1(a). The temperature is capable to reduce strong intermolecular interaction, which the aggregation of liquid can be avoided. When this temperature is reduced, the intermolecular interaction will force the molecules of liquid to form self-assemble as in Figure 1(b). Due to the interaction of self-assembly, it actually produces a thin fibre in one dimension. As the time varies, this fibre is growing and producing bundles of thin fibres, which minimize the movement of molecules of liquid as depicted in Figure 1(c). Then, over a certain time period, these bundles of thin fibres grow to form the formation of a 3D-network, which is also recognized as the formation of a gel as illustrated in Figure 1(d).

The first concern is on the preparation process of samples prior to the measurement in the laboratory. One of the cases that needs to be considered when producing samples for this phantom is the preparation method. Different preparation methods could result in different sets of measurement data. This can be explained by two gelatine-based samples with same composition but prepared by different methods as follows.

One of the samples is the mixture of gelatine and hot water that are stirred until gelatine is dissolved completely. The preparation for the second sample is almost similar but during the mixture preparation, it is heated. These different preparation methods affect the dielectric measurement results, which the first sample has lower permittivity compared to the second sample. This effect is related to the condition of water at different temperatures. At low temperature, water can turn to solid, which called freezing process and forming an ice. The increase of temperature over 0°C turns the ice into liquid and when the liquid is heated at boiling point at 100°C (universal boiling point), it turns to gas which is known as evaporation process. Different conditions of water resulting different density and weigh. Molecules of water at higher temperatures separate farther apart compared to lower temperatures. It explains that water at lower temperatures has closer molecules and higher density and vice versa at higher temperatures. For that matter, the difference in molecule condition of water at respective temperatures affects the permittivity of sample that is produced at different temperature levels, which water at higher temperature has higher permittivity, then decrease respectively at lower temperature [28].

The preparation of samples in this article, i.e the specific ingredients for each sample, is first defined. Then, the sample is produced by adding gelatine, jelly and/or sugar with a specific ratio into water. The mixture is then heated until all materials are dissolved. Then, the mixture is cooled down to form a semisolid. The semisolid samples are ready for dielectric measurements. All samples in this article are prepared using this procedure to ensure that the preparation method will not affect the dielectric results for each sample.

Since the dielectric properties of material are temperature dependent, so it is important to consider the effects of temperature before the measurement is conducted. All the measurements presented in this article are conducted at room temperature, which approximately at 23ºC. This temperature is chosen in order to simplify the challenge to control the temperature of samples during measurements. Stable temperature in closed room reduces the variation of temperature that might occur during measurement procedure. The dielectric properties are basically not only temperature dependent but also frequency dependent. Lower frequency will allow higher penetration of signal, which results in higher permittivity level and vice versa for the higher frequency. This explains the trend observed from the plotted data of permittivity that is inversely proportional to the frequency. Apart from the frequency and temperature, the dielectric properties of material also depend on their composition of ingredients. In the research reported in [29], other than temperature, the addition of ancillary material, for example, sugar also changes the dielectric properties. The gelatine and water, which are used in this article also provide a variation on dielectric properties based on their mixture ratio. So, when preparing phantom all these properties can be taken under consideration to optimise the dielectric properties of phantom. Although the temperature of normal human body is around 36.5-37.5 °C [30] and the theoretical dielectric properties of human body tissues in [26] is measured at 37 °C, but with suitable composition of ingredients in the phantom, the dielectric properties of human tissues at 37 °C can be represented by the phantom at room temperature or any specific temperature as suggested.

Basically, there are many different types of materials that have been tested in order to imitate the properties of the concerned tissues over the desired frequency range of 1 to 6 GHz. Table 1 shows the selected samples with the compositions used in the experiment to mimicking grey matter, white matter, cerebral spinal fluid (CSF), blood and skin tissues, accordingly.

Table 1 Composition of grey matter, white matter, cerebral spinal fluid (CSF), blood and skin phantom samples in gram (g)

Material	Grey Matter Samples (g)		White Matter Samples (g)		Cerebral Spinal Fluid Samples (g)		Blood Samples (g)		Skin Samples (g)	
	Sample 1	Sample 2	Sample 3	Sample 4	Sample 5	Sample 6	Sample 7	Sample 8	Sample 9	Sample 10
Jelly Powder	-	-	10	-	-	10	-	10	-	-
Gelatine	5	5	-	5	10	-	10	-	10	10
Sugar	0.5	-	-	-	-	-	-	-	-	-
Water (ml)	20	10	10	14	50	40	30	30	20	15

5.0 MEASUREMENT RESULTS

The experimental results of materials are obtained via an open-circuited coaxial technique. The dielectric measurements of each material are initially assessed over a frequency range of 1 to 6 GHz by using a vector network analyser (VNA). The configuration of the measurement setup for testing dielectric properties of materials is shown in Figure 2. The ultimate goal is to determine a composition of materials and substances that can perform similar relative permittivity and conductivity as a real grey matter, white matter, cerebral spinal fluid (CSF), blood and skin tissues. In this experiment, more than a hundred samples have been tested and from Table 1, 10 of them are selected due to the best performance of relative permittivity and conductivity properties, which are quite similar to real human brain tissues.

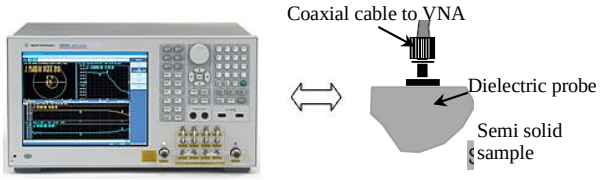

Figure 2A measurement setup for the testing of electrical properties with a vector network analyser (VNA) and dielectric probe

At this point, a number of experiment results are presented, which can be the key to model a realistic human head phantom for the purpose of a microwave imaging system. As discussed earlier, all the selected materials as the compositions detailed in Table 1 have a potential to have similar behaviour as real human head tissues in terms of relative permittivity and conductivity. Figures 3 to 7 show the relative permittivity and conductivity plots of grey matter, white matter, cerebral spinal fluid, blood and skin samples. Samples P1 to P10 represent the data of permittivity, while Samples C1 to C10 represent the data of conductivity for Samples 1 to 10. Also included in the graphs are theoretical data as obtained from [26].

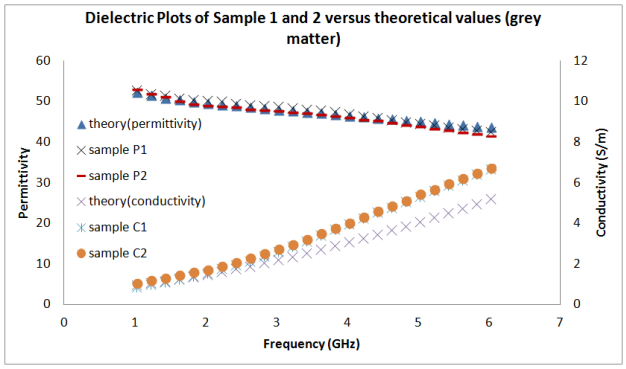

Figure 3 Relative permittivity and conductivity of Sample 1 and 2 versus theoretical values of grey matter

From observation on relative permittivity plots in Figure 3, the theoretical and measured data of Sample 1 and 2 of grey matter are quite similar. The observation at each point shows that Sample 1 of grey matter is a slightly higher than Sample 2. Hence, Sample 2 has closer relative permittivity to the theoretical data than Sample 1. While, the conductivity data plotted in Figure 3 shows a significant different between theoretical data and calculated data for Samples 1 and 2 of grey matter at frequency range between 3 and 6 GHz. In contrast, both samples have greater similarity to the theoretical data across the frequency range between 1 and 3 GHz.

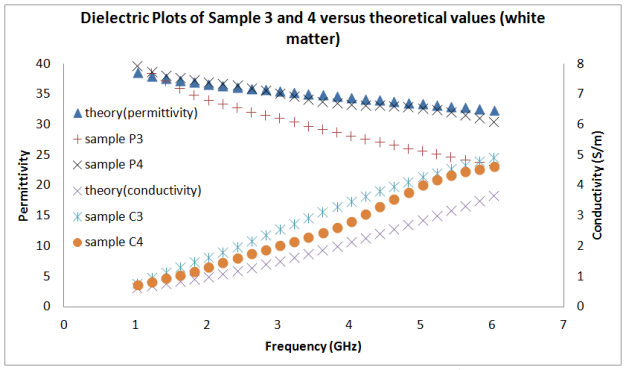

Figure 4 Relative permittivity and conductivity of Samples 3 and 4 versus theoretical values of white matter

Meanwhile, the relative permittivity plots in Figure 4 present a significant different between Samples 3 and 4 of white matter. It clearly shows that the relative permittivity data for Sample 4 is more similar to the theoretical data compared to Sample 3. While, the conductivity data plotted in Figure 4 shows each sample and theoretical data have slightly different conductivity level. The lower value exhibits by the data of Sample 4, while the highest data is indicated by Sample 3. This condition on the conductivity plot shown that Sample 4 of white matter exhibits better similarity to the theoretical data compared to Sample 3.

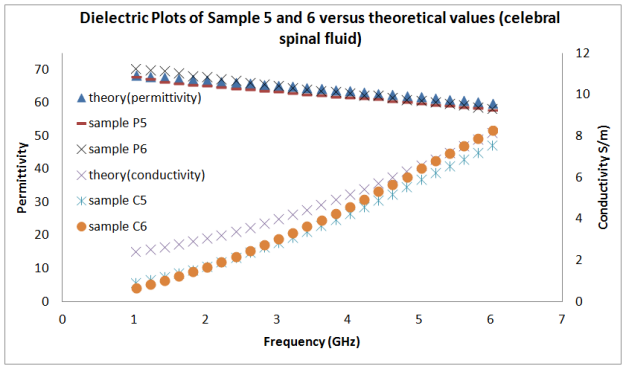

Figure 5 Relative permittivity and conductivity of Samples 5 and 6 versus theoretical values of cerebral spinal fluid (CSF)

The relative permittivity plots in Figure 5 depict the theoretical and measured data of Samples 5 and 6 of cerebral spinal fluid (CSF) which are quite comparable. Each point of plots indicates that Sample 6 is closer to the theoretical averagely. Sample 6 data are plotted consistently close to theoretical data with small difference, which in contrast for Sample 5 with lower relative permittivity than theoretical data can be noted. While, the conductivity data as plotted in Figure 5 shows that each sample has lower conductivity than theoretical data. However, Sample 6 of cerebral spinal fluid (CSF) is noted to be closer to theoretical data, especially at frequency between 4 and 6 GHz.

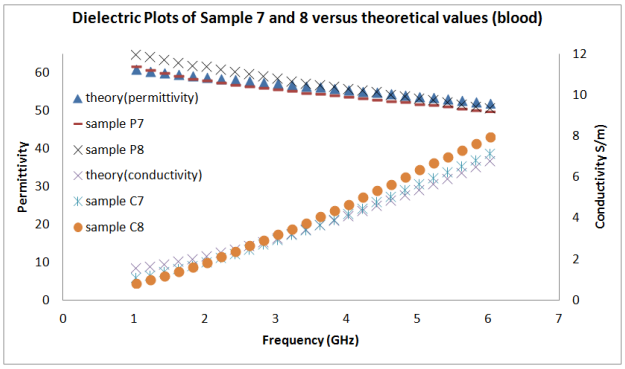

Figure 6 Relative permittivity and conductivity of Samples 7 and 8 versus theoretical values of blood

From the observation on relative permittivity plots in Figure 6, the theoretical and measured data of Samples 7 and 8 of blood are relatively comparable. However, it is clearly seen that the data for sample 7 is closer to the theoretical data at every point compared to Sample 8 which only similar at frequency range between 3 and 6 GHz. Repeating trend of its permittivity plots, its conductivity plots on Figure 6 also show that data for sample 7 is closer to the theoretical data averagely compared to Sample 8.

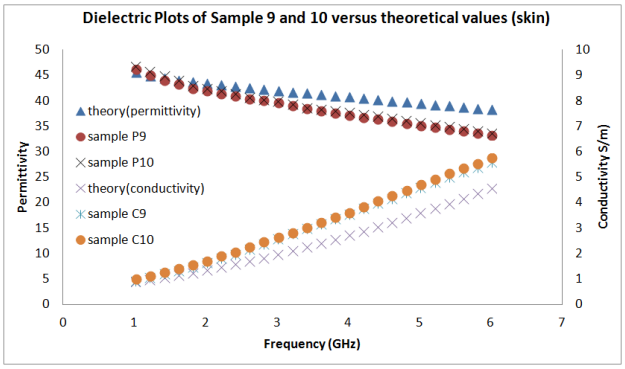

Figure 7 Relative permittivity and conductivity of Samples 9 and 10 versus theoretical values of skin

Whilst, by referring to the relative permittivity plots in Figure 7, both phantom samples of skin demonstrate similar permittivity level which the highest is around 47 at 1 GHz and decrease to around 34 at 6 GHz. the observation for conductivity data plotted in Figure 7, however, depicts a difference between calculated data and theoretical data of skin, which obtained data is slightly higher than theoretical data. However, the data for Sample 10 is slightly higher than the data for sample 9, which simply makes the data for Sample 9 closer to theoretical data.

6.0 ANALYSIS OF SAMPLES

A few of gelatine-based and jelly-based samples have been measured for their dielectric properties. From the observation on plotted data of 10 samples from Figures 3 to 7, data for each sample then was summarized in terms of its percentage of relative permittivity error between measurement and theoretical data as presented in Table 2. The value of error, S$i\Delta$ (where, i =1 to 10) is the difference between measurement data and theoretical data as expressed in the following Equation (5):

$$Si\Delta(\%) = \frac{|\text{theory} - \text{measurement}|}{\text{theory}} \times 100\% \quad (5)$$

Referring to the summarized data in Table 2, the selection of samples which are closer to theoretical data can be made easier based on its percentage of average error. Lowest percentage indicates the closest phantom characteristic to mimic the real human brain tissue, which represented by its theoretical data. Average relative permittivity errors for Samples 1 and 2 of grey matter are 1.27% and 1.80%, respectively. Where, Sample 1 has lower average relative permittivity error than Sample 2 by 0.53% which makes Sample 1 more similar and suitable for grey matter tissue. For white matter tissue, however, Sample 4 with 2.20% error shows a smaller variation, which is 12.69% lower than Sample 3. Meanwhile, Sample 6 of cerebral spinal fluid (CSF) phantom resulting in lower error compared to Sample 5 with 1.36% difference. While, Sample 7 and 8 for blood show only a little difference, which Sample 8 is 0.28% lower than Sample 7.This indicates Sample 8 is more similar to the theoretical data of blood. The last two samples of Samples 9 and 10 of skin show an error difference of 0.86%, which sample 10 is the lower one. Therefore, Sample 10 exhibits better similarity to the theoretical data of skin.

Besides the relative permittivity, the conductivity is also taken under consideration during sample selection. Table 3 shows the percentage of conductivity error obtained using Equation (5) between measurement and theoretical data for Samples 1 to 10. From Table 3, average error for Samples 1 and 2 of grey matter samples are 20.21% and 23.40%, respectively. Hence, Sample 1 has 3.19% lower error than Sample 2. For white matter phantom samples, Sample 3 has a higher error of 55.68% compared to Sample 4 with 31.87% that results in 23.81% difference between both samples. Conductivity of Samples 5 and 6 for CSF shows that Sample 6 with error of 23.85% is lower than Sample 5 by 3.66%. While, Sample 7 and Sample 8 show 8.02% difference, which Sample 7 with the error of 8.27 is the lower one. And for skin phantom samples, Sample 9 with the error of 25.89% is the lower one compared to Sample 10 with the error of 29.40% which results in a difference of 3.51%.

The observation on both Tables 2 and 3 show that Sample 1 with average relative permittivity and conductivity error of 1.27% and 20.21%, is more suitable to mimic grey matter tissue compared to Sample 2. While, Sample 4 is decided to be more appropriate for white matter tissue since its relative permittivity and conductivity is closer to theoretical value compared to Sample 3. For CSF, Sample 6 is closer to theoretical data based on its both relative permittivity and conductivity with average error of 1.59% and 23.85%. For blood, the analysis on relative permittivity shows that Sample 8 with 2.57% error is closer to theoretical value compared to Sample 7 with 2.85% error, but the conductivity shows that sample 7 is closer to theoretical value with 8.27% error compared to sample 8 with 16.29% error. This condition indicates that both Samples could be selected, so the selection then is relied on the error difference between Samples 7 and 8. The relative permittivity shows an error difference of 0.28% and the conductivity of 8.02%. Since the relative permittivity has only a small difference, so selection is based on conductivity, which Sample 7 is decided fit to mimic the blood. Repeating the comparison as Sample 7 and 8, the next two samples of Samples 9 and 10 for skin, are seen to have an identical issue. The analysis on relative permittivity shows that Sample 10 with 6.38% error is more comparable to theoretical value compared to Sample 9 with 7.24% error. In contrast, the conductivity demonstrates that Sample 9 has a lower error of 25.89% compared to Sample 10 with 29.40% error. The relative

permittivity and the conductivity exhibit the error difference of 0.86% and 3.51%. Hence, since the relative permittivity has a small difference, so the selection is based on conductivity. Therefore, Sample 9 is fit to mimic the skin tissue.

Referring to the analysis and observation, the permittivity of presented samples is linearly proportional to the permittivity of water. The relative permittivity of water is approximately around 80 at 1 GHz, which shows a decrement to 70 at higher frequency of 6 GHz. The addition of jelly or gelatine into water then bonds the molecules of water, which changes the water physical condition from a liquid to a semisolid. The bonding of water molecules causes the decrement of relative permittivity but still similar to its original trends.

This condition is proven by the measurement of two gelatine-based samples, which are Samples 5 and 7 as plotted in Figures 4 and 5, respectively. Sample 5 is composed of 10 g gelatine and 50 g water, which has the relative permittivity that inversely proportional to frequency of 68 at 1 GHz frequency and decrease to 56 at 6 GHz. Sample 7 was produced by 10g of gelatine and 30g of water resulting in similar relative permittivity trend with relative permittivity of Sample 5 but at lower value, which is 62 at 1 GHz and decrease to 50 at 6 GHz.

Two samples have been tested for every grey matter, white matter, cerebral spinal fluid, blood, and skin tissues. The experiment results shown five samples of Sample 1, Sample 4, Sample 5, Sample 7, and Sample 10 almost meet the real characteristics of grey matter, white matter, cerebral spinal fluid (CSF), blood, and skin, respectively.

In composition of Sample 1, sugar has been added besides gelatine and water. The composition of Sample 1 contains 20g of water, while Sample 2 contains 10 g of water. From the theory mentioned earlier, Sample 1 that contains a higher amount of water should have higher relative permittivity compared to Sample 2, which has a lower amount of water. But the results that were presented in Figure 2 shows that these two samples have similar relative permittivity. This condition indicates that the addition of 0.5 g of sugar has reduced the relative permittivity of Sample 1 to be similar with the relative permittivity of Sample 2. Therefore, it is proven that the addition of sugar would decrease the relative permittivity.

From the results and analysis of samples in this article, the relative permittivity of samples can be affected by the amount of water. The addition of water will increase the relative permittivity of sample and vice versa if the amount of water is reduced. But, the addition and reduction of the amount of water was also able to change the physical condition of sample, which the addition of water makes the sample has less solidity and the reduction in amount of water produced a sample with better solidity shape. Besides water, sugar also plays a role in changing the relative permittivity of material, which as mentioned earlier, sugar can be used to reduce the relative permittivity of material.

In the experiment presented in this article, gelatine has been found to be the most suitable substance to mimicking the real human head tissues. In a certain composition, gelatine has the characteristics, which almost similar to the real grey matter, white matter cerebral spinal fluid, blood, and skin tissues rather than jelly powder. The analysis in the experiment can be used to produce other samples for each cell and tissue in the human brain by varying the composition of the sample in the correct ratio.

Table 2 The percentage of relative permittivity error between measurement and theoretical data for Sample 1 to 10

Frequency	Grey Matter Samples		White Matter Samples		CSF Samples		Blood Samples		Skin Samples	
(GHz)	ΔS1 (%)	ΔS2 (%)	ΔS3 (%)	ΔS4 (%)	ΔS5 (%)	ΔS6 (%)	ΔS7 (%)	ΔS8 (%)	ΔS9 (%)	ΔS10 (%)
1	1.07	1.23	3.86	2.87	0.83	2.76	1.18	6.40	1.11	2.44
2	1.14	1.34	7.09	0.83	2.61	1.48	1.73	4.70	3.47	2.40
3	1.68	0.62	12.23	0.99	3.02	0.18	2.76	2.30	5.74	5.23
4	1.05	1.17	17.98	3.12	3.27	1.27	3.45	0.60	8.94	7.52
5	0.97	2.91	23.04	2.12	3.33	2.06	3.88	1.01	11.13	9.91
6	2.55	5.10	27.68	5.77	3.59	2.98	4.37	2.66	13.38	12.23
Δave	1.27	1.80	14.89	2.20	2.95	1.59	2.85	2.57	7.24	6.38

Table 3 The percentage of conductivity error between measurement and theoretical data for Sample 1 to 10

Frequency	Grey Matter Samples		White Matter Samples		CSF Samples		Blood Samples		Skin Samples	
(GHz)	ΔS1 (%)	ΔS2 (%)	ΔS3 (%)	ΔS4 (%)	ΔS5 (%)	ΔS6 (%)	ΔS7 (%)	ΔS8 (%)	ΔS9 (%)	ΔS10 (%)
1	9.81	7.26	25.43	17.11	62.16	72.02	30.04	47.91	5.37	11.56
2	4.33	13.51	63.55	31.59	44.76	45.03	13.71	15.73	22.52	27.92
3	18.96	22.63	69.89	33.71	28.57	24.26	3.13	4.50	32.17	34.80
4	29.44	30.08	62.47	32.07	18.56	11.67	1.78	12.58	31.46	33.27
5	30.84	32.31	49.72	40.24	10.91	2.18	5.06	17.46	28.67	31.49
6	28.20	28.46	34.33	26.15	7.76	1.27	5.17	16.65	22.72	26.27
Δave	20.21	23.40	55.68	31.87	27.51	23.85	8.27	16.29	25.89	29.40

7.0 CONLUSION

A human head phantom characterization based on the study of its electrical properties across 1 to 6 GHz has been presented. The study has shown that the human head phantom can be modelled using simple and common materials available in the market, which are jelly powder, gelatine, water and sugar. From the conducted experiments, it has been found that gelatine is the most suitable substance in mimicking real human head tissues. Where, by having certain amount gelatine and water, tissue of grey matter, white matter cerebral spinal fluid, blood, and skin can be modelled. By having the phantom with similar electrical properties to real human head, further study can be performed in microwave imaging application and system.

Acknowledgement

The authors are grateful to the Ministry of Higher Education Malaysia (MOHE) and Universiti Teknologi Malaysia (UTM) for financial assistance via Fundamental Research Grant

Scheme (FRGS) with Vote Number of 4F206, Research University Grant (GUP) with Vote Number of 05H43, and UTM Zamalah Award.

References

[1] Q. Fang. 2004. Computational Methods for Microwave Medical Imaging. Ph.D. Dissertation. Dartmouth College, Hanover.

[2] H. Trefna and M. Persson. 2008. Antenna Array Design for Brain Monitoring. *Antennas and Propagation Society International Symposium.* 1–4.

[3] S. Y. Semenov, R. H. Svenson, V. G. Posukh, A. G. Nazarov, Y. E. Sizov, A. E. Bulyshev, A. E. Souvorov, W. Chen, J. Kasell, and G. P. Tatsis. 2002. Dielectrical Spectroscopy of Canine Myocardium During Acute Ischemia and Hypoxia at Frequency Spectrum from 100 kHz to 6 GHz. *IEEE Transactions on Medical Imaging.* 21(6).

[4] R. Gagarin, N. Hyoung-sun Youn Celik and M. Iskander. 2010. Noninvasive Microwave Technique for Hemodynamic Assessments. *Antennas and Propagation Society International Symposium (APSURSI).* 1–4.

[5] D. Ireland and M. Bialkowski. 2010. Feasibility Study on Microwave Stroke Detection Using a Realistic Phantom and the FDTD Method. *2010 Asia-Pacific Microwave Conference Proceedings (APMC)*. 1360–1363.

[6] Alshehri, S. A., S. Khatun. 2009. UWB Imaging for Breast Cancer Detection Using Neural Networks. *Progress In Electromagnetic Research C*. 7: 79–93.

[7] AlShehri, S. Khatun, A. B. Jantan, R. S. A. Raja Abdullah, R. Mahmood, and Z. Awang. 2011. Experimental Breast Tumor Detection using NN-based UWB Imaging. *Progress In Electromagnetics Research*. 111: 447–465.

[8] N. Seman and M. E. Bialkowski. 2006. Design of a Wideband Reflectometer for a Microwave Imaging System. *International Conference on Microwaves, Radar & Wireless Communications (MIKON)*. 25–28.

[9] Bindu, G., S. J. Abraham, A. Lonappan, V. Thomas, C. K. Aanandan, and K. T. Mathew. 2006. Active Microwave Imaging for Breast Cancer Detection. Progress in Electromagnetics Research. *PIER*, 58: 149–169.

[10] H. Zhang, S. Y. Tan, and H. S. Tan. 2008. A Novel Method for Microwave Breast Cancer Detection. *Progress In Electromagnetics Research*. 83: 413–434.

[11] V. Zhurbenko. 2011. Challenges in the Design of Microwave Imaging Systems for Breast Cancer Detection. *Advanced in Electrical and Computer Engineering*. 11(1).

[12] E. C. Fear, X. Li, S. C. Hagness and M. A. Stuchly. 2002. Confocal Microwave Imaging for Breast Cancer Detection: Localization of Tumors in Three Dimensions. *IEEE Transactions on Biomedical Engineering*. 49(8).

[13] J. C. Y. Lai, C. B. Soh, E. Gunawan, and K. S. Low. 2010. Homogeneous and Heterogeneous Breast Phantoms for Ultra-Wideband Microwave Imaging Applications. Progress In Electromagnetics Research. *PIER 100*. 397–415.

[14] M. E. Bialkowski, N. Seman, A.Abbosh and W. C. Khor. 2006. Compact Reflectometers for a Wideband Microwave Breast Cancer Detection System. *African Journal of Information and Communication Technology*. 2(3): 119–125.

[15] Jae Myeong Choi,Heau-Jo Kang, Yong-Seok Choi. 2008. A Study on the Wireless Body Area Network Applications and Channel Models. *Future Generation Communication and Networking (FGCN) '08 Second International Conference.* 2: 263–266.

[16] F. Martell, C. Buratti and R. Verdone. 2011. On the Performance of an IEEE 802.15.6 Wireless Body Area Network. *11th European Wireless Conference 2011-Sustainable Wireless Technologies (European Wireless)*. 1–6.

[17] S. Y. Semenov and D. R. Corfiled. 2008. Microwave Tomography for Brain Imaging: Feasibility Assessment for Stroke Detection. *International Journal of Antennas and Propagation*. Article ID 254830. 8 pages.

[18] I. A. Gouzouasis and I. S. Karanasiou and N. K. Uzunoglu. 2009. Exploring the Enhancement of the Imaging Properties of a Microwave Radiometry Systems for Possible Functional Imaging Using a Realistic Human Head Model. *4th International Conference Imaging Technology in Bio Medical Sciences*. Medical Images to Clinical Information–Bridging the Gap.

[19] M. Miyakawa, Y. Kawada and M. Bertero. 2005. Image Generation in Chirp Pulse Microwave Computed Tomography (CP-MCT) by Numerical Computational: Computational of a Human Head Model. *Electronics and Communications in Japan Part 3*. 88(9).

[20] I. S. Karanasiou, N. K. Uzunogle and A. Garetsos. 2004. Electromagnetic Analysis of Non-Invasive 3D passive Microwave Imaging System. Progress in Electromgnetics Research. *PIER*. 44: 287–308.

[21] D. Ireland and M. Bialkowski. 2010. Feasibility Study on Microwave Stroke Detection Using a Realistic Phantom and the FDTD Method. *Asia Pacific Microwave Conference*. 1360–1363.

[22] D. Ireland and M. Bialkowski. 2011. Microwave Head Imaging for Stroke Detection. *in Electromagnetics Research M*. 21: 163–175.

[23] K. S. Kwak, S. Ullah and N. Ullah. 2010. An Overview of IEEE 802.15.6 Standard. *2010 3rd International Symposium on Applied Sciences in Biomedical and Communication Technologies (ISABEL)*. 1–6.

[24] A. Oikonomou, I. S. Karanasiou and N. K. Uzunoglu. 2010. Phased-Array Near Field Radiometry for Brain Intracranial Applications. *Progress in Electromagnetics Research*. 109: 345–360.

[25] D. Miklavcic and N. Pavselj. 2006. Electric Properties of Tissues. *Wiley Encyclopaedia of Biomedical Engineering*. New York: John Wiley & Sons.

[26] Dielectric Properties of Body Tissues In The Frequency Range of 10Hz – 100 GHz, Available: http://niremf.ifac.cnr.it/tissprop/, [Accessed: December 3rd, 2013].

[27] KimmoLeivo. 2011. Gelation and Gel Properties of Two- and Three-Component Pyrene Based Low Molecular Weight Organogelators. Ph.D. Dissertation. Department of Chemistry. University Of Jyväskylä.

[28] Lech RUSINIAK. 2004. Electric Properties of Water. *Institute of Geophysics*. Polish Academy of Sciences Poland. 52(1).

[29] Said, M. S. and Seman. N. 2013. Investigation on Dielectric Variation Factors in Materials for Brain Phantom. *IEEE Student Conference on Research and Development*. 281–285.

[30] Karakitsos D, Karabinis. 2008. Hypothermia Therapy After Traumatic Brain Injury in Children. *N. Engl. J. Med*. 359(11): 1179–80.

[31] Mohammed, B. Abbosh, A. Henin, B. Sharpe, P. 2012. Head Phantom for Testing Microwave Systems for Head Imaging. *Cairo International Biomedical Engineering Conference (CIBEC)*. 191–193.

[32] Mohammed, B. J. Abbosh, A. M. Mustafa, S. Ireland, D. 2014. Microwave System for Head Imaging. *IEEE Transactions on Instrumentation and Measurement*. 63: 117–123.